Coulomb distortion measurements by comparing electron and positron quasielastic scattering off ^{12}C and ^{208}Pb

P. Guèye,* M. Bernheim, J. F. Danel, J. E. Ducret, L. Lakéhal-Ayat, J. M. Le Goff, A. Magnon, C. Marchand, J. Morgenstern, J. Marronclе, P. Vernin, and A. Zghiche-Lakéhal-Ayat†
DAPNIA, Service de Physique Nucléaire, CEA-Saclay, F-91191 Gif-Sur-Yvette, Cedex, France

V. Breton
Laboratoire de Physique Corpusculaire, Université Blaise Pascal, Institut de Physique Nucléaire et de Physique des Particules, F-63177 Aubière, Cedex, France

S. Frullani, F. Garibaldi, F. Ghio, and M. Iodice
Laboratorio di Fisica, Istituto Superiore di Sanità e Istituto di Fisica Nucleare, Sezione Sanità, I-00161 Roma, Italy

D. B. Isabelle‡
Centre d'Etudes et de Recherche par Irradiation, Centre National de la Recherche Scientifique, F-45071 Orléans, Cedex 02, France

Z.-E. Meziani
Department of Physics, Temple University, Philadelphia, Pennsylvania 19122

E. Offermann§
Thomas Jefferson National Accelerator Facility (TJNAF), 12000 Jefferson Avenue, Newport News, Virginia 23606

M. Traini
Dipartimento di Fisica, Università degli Studi di Trento, I-38050 Povo (Trento), Italy and INFN, G.C. Trento, Italy

(Received 17 May 1999; published 8 September 1999)

Positron and electron quasielastic cross sections on ^{12}C and ^{208}Pb were measured at the Saclay linear accelerator (ALS) to test Coulomb corrections to the plane-wave Born approximation. The positron and electron response functions at the same effective kinematics were found to be equal within a 3% experimental uncertainty, which allows us to discriminate between different theoretical models of Coulomb distortions. Our result strongly supports the effective momentum approximation, even for nuclei as heavy as ^{208}Pb. [S0556-2813(99)01210-8]

PACS number(s): 25.30.Hm, 25.70.Bc, 27.20.+n, 27.80.+w

I. INTRODUCTION

Accurate electron-scattering experiments allow us to get unique information about nuclear structure. In the last few decades, quasielastic scattering measurements had a strong impact on our knowledge of the single-particle and many-particle nuclear properties such as momentum distributions, two-body densities, spectroscopic factors, and spectral functions. While many aspects have been understood, such as the existence of a shell structure, or the relevance of short-range correlations, meson exchange currents, and of isobar configurations, others remain unsolved such as the quenching of the longitudinal response in inclusive scattering and the low value of the spectroscopic factors measured in $(e,e'p)$ reactions. In order to disentangle nuclear structure from off-shell single nucleon effects, such as the modification of the electromagnetic properties of bound nucleons, it is important to study the mass dependence of such effects. The study of these remaining aspects requires much effort from both the theoretical and the experimental points of view, and they are part of the physics issues that are addressed with the new high duty cycle accelerators.

The experimental study of inclusive as well as exclusive reactions induced by electrons has an intrinsic limitation when the charge of the target nucleus is large: Coulomb distortions become sizeable and the electron-wave functions cannot be approximated by plane waves. In the case of elastic scattering, the problem was solved by using a phase-shift analysis of the cross section, and recent experiments [1,2] tested the validity of the method with great accuracy by comparing electron and positron cross sections. The present paper reports on a similar experiment [3] performed in the quasielastic region for the first time.

A large theoretical effort has been made in the last ten years to understand the role of Coulomb distortion effects in

*Present address: Hampton University, Nuclear/High Energy Physics Research Center, Hampton, VA 23606.
†Present address: Center de Recherches Nucléaires Cronenbourg, F-67037 Strasbourg, Cédex, France.
‡Deceased.
§Present address: Renaissance Technologies Corp., 600 Rt. 25A, East Setauket, NY 11733.

$(e,e'p)$ as well as (e,e') quasielastic reactions. In particular, the effect of Coulomb distortions on the evaluation of spectroscopic factors have been discussed both within nonrelativistic [4,5] and relativistic [6–9] frameworks. The literature on Coulomb corrections to inclusive reactions is ample and includes nonrelativistic [10–12] as well as relativistic [13,14] treatments of the nuclear wave functions.

In principle, the problem can be solved within a complete distorted-wave Born approximation (DWBA) for quasielastic scattering [10,13]. However, this calculation is extremely computer time consuming for inclusive processes. In order to have a more practical procedure, few approximations have been proposed [11,12,14,15] with a particular emphasis on their validity in the separation of the cross section into its longitudinal and transverse components.

The most common and simple way to describe the quasielastic inclusive scattering of charged leptons with nuclei is the plane-wave Born approximation (PWBA). Here only one (hard) virtual photon is exchanged between the target nucleus and the leptonic probe. In the PWBA, the incoming and outgoing leptons are described by plane waves and the cross section assumes the well-known form:

$$\left.\frac{d^3\sigma}{d\Omega_{e'}\,dE_{e'}}\right|^{\mathrm{PWBA}} = \sigma_{\mathrm{Mott}}\left\{\left(\frac{Q^2}{\mathbf{q}^2}\right)^2 R_L(|\mathbf{q}|,\omega) + \left(\frac{Q^2}{2\mathbf{q}^2}+\tan^2\frac{\theta}{2}\right)R_T(|\mathbf{q}|,\omega)\right\} = \sigma_{\mathrm{Mott}}\times S_{\mathrm{total}}(|\mathbf{q}|,\omega,\theta) \tag{1}$$

with

$$\sigma_{\mathrm{Mott}} = 4\alpha^2\cos^2(\theta/2)E_{e'}^2/Q^4, \tag{2}$$

and

$$Q^2 = -q^2 = 4E_eE_{e'}\sin^2(\theta/2), \quad \omega = E_e - E_{e'},$$
$$\mathbf{q}^2 = Q^2+\omega^2, \quad \mathbf{q} = \mathbf{k_e} - \mathbf{k_{e'}}. \tag{3}$$

Here $(\mathbf{k_e},E_e)$, $(\mathbf{k_{e'}},E_{e'})$, and $(\mathbf{q},\omega)$ are the four momenta of the incoming electron, the outgoing electron and the virtual photon, respectively; θ is the scattering angle, $S_{\mathrm{total}}(|\mathbf{q}|,\omega,\theta)$, $R_L(|\mathbf{q}|,\omega)$, $R_T(|\mathbf{q}|,\omega)$ are the total, longitudinal, and transverse response functions, respectively. The mass of the projectile has been neglected in the high-energy approximation.

In PWBA the cross section does not depend on the charge of the probe, thus the electron and positron cross sections are equal. However, PWBA cannot be applied to heavy nuclei where nuclear charge effects become sizeable. The first Coulomb correction terms to the Born series are related to the energy increase (decrease) of the incident and the scattered electron (positron) due to the nuclear Coulomb potential; E_e and $E_{e'}$ are replaced by $E_{e,\mathrm{eff}} = E_e - V_C$ and $E_{e',\mathrm{eff}} = E_{e'} - V_C$, where V_C is the value of the effective Coulomb potential energy seen by the lepton during the scattering process. It is assumed to have a constant negative value[1] for electrons and positive value for positrons.

In addition, the normalization of the lepton wave function is altered because of current conservation and reads [16]

$$\chi(\mathbf{r}) \simeq \frac{|\mathbf{k}_{\mathrm{eff}}|}{|\mathbf{k}|}e^{i\mathbf{k}_{\mathrm{eff}}\cdot\mathbf{r}}, \tag{4}$$

where

$$\mathbf{k}_{\mathrm{eff}} = \mathbf{k}\left(1-\frac{V_C}{|\mathbf{k}|}\right). \tag{5}$$

The momentum transfer $\mathbf{q}$ is replaced by an effective momentum transfer $\mathbf{q}_{\mathrm{eff}} = \mathbf{k}_{e,\mathrm{eff}} - \mathbf{k}_{e',\mathrm{eff}}$, and Q^2 is replaced by $Q^2_{\mathrm{eff}} = 4E_{e,\mathrm{eff}}E_{e',\mathrm{eff}}\sin^2(\theta/2)$. Since E_e and $E_{e'}$ are modified by the same amount, the energy transfer ω remains unchanged. Within this approximation, called the effective momentum approximation (EMA), the cross section can be written

$$\left.\frac{d^3\sigma}{d\Omega_{e'}\,dE_{e'}}\right|^{\mathrm{EMA}} = \sigma_{\mathrm{Mott}}\left\{\left(\frac{Q^2_{\mathrm{eff}}}{\mathbf{q}^2_{\mathrm{eff}}}\right)^2 R_L(|\mathbf{q}_{\mathrm{eff}}|,\omega) + \left(\frac{Q^2_{\mathrm{eff}}}{2\mathbf{q}^2_{\mathrm{eff}}}+\tan^2\frac{\theta}{2}\right)R_T(|\mathbf{q}_{\mathrm{eff}}|,\omega)\right\} = \sigma_{\mathrm{Mott}}\times S_{\mathrm{total}}(|\mathbf{q}_{\mathrm{eff}}|,\omega,\theta), \tag{6}$$

where σ_{Mott} is still given by Eq. (2) because of the flux normalization terms of Eq. (4) (see Ref. [20]).

The expression of the effective momentum transfer is

$$\mathbf{q}_{\mathrm{eff}} = \mathbf{q}\left(1-\frac{V_C}{E_e}\right) - \omega\frac{V_C}{E_e}\hat{\mathbf{k}}_{e'}, \tag{7}$$

where $\hat{\mathbf{k}}_{e'}$ is the unit vector in the direction of the scattered lepton. The value of $\mathbf{q}_{\mathrm{eff}}$ depends on the incident lepton charge through the sign of the potential energy term V_C, and $\mathbf{q}_{\mathrm{eff}}$ is *not* aligned along the momentum $\mathbf{q} = \mathbf{k}_e - \mathbf{k}_{e'}$ except in the case of *elastic* scattering where $\omega \approx 0$. The main effect of the EMA is a shift of the quasielastic peak due to the energy change of the incident and scattered lepton: $\omega_{\mathrm{peak}} \approx Q^2_{\mathrm{eff}}/2M_p$, where M_p is the proton mass.

If EMA is a good approximation, we must obtain the same total response function for positrons at an incident energy E_{e^+} and for electrons at an incident energy $E_{e^-} = E_{e^+} - 2|V_C|$. The exact value of V_C is unknown and has to be determined experimentally. In addition to such first-order effects, the cross section for heavy nuclei is modified in am-

[1]More rigorously one should treat the effective momentum as a *local* quantity [17,18]; but from an experimental point of view we will treat V_C as an effective parameter related to an *average* value of the Coulomb potential as seen by the incoming and outgoing leptons.

plitude by higher-order corrections known as focusing due to the distortion of the wave front.

We present in this paper the first experimental check of the validity of the EMA for quasielastic electron scattering and we estimate the significance of higher-order corrections. The experimental setup is described in Sec. II A and radiative corrections in Sec. II B. Section III A describes the experimental procedure used to extract Coulomb distortion effects, in particular the value of V_C, from the electron and positron data. In Sec. III B we present our experimental results and compare them to the available theoretical predictions in Sec. III C. Conclusions are drawn in Sec. IV.

II. THE EXPERIMENT

This experiment was performed at the 700 MeV Saclay Linear Accelerator (ALS) which provided a 30 nA positron beam with energy up to 600 MeV and $\Delta E/E$ of 2×10^{-3}. The scattered particles were detected in the HE1 (electron-positron) hall. Electron and positron cross sections were measured at two kinematics ($E_e=420$ MeV, 60°) and (262 MeV, 143°) for ^{208}Pb and one kinematic (420 MeV, 60°) for ^{12}C.

A. Experimental setup

1. Targets

Three different targets were used: a natural carbon target (500 mg/cm^2) and two ^{208}Pb targets (101 and 168 mg/cm^2) of isotopic purity better than 99%. The targets consisted of plane foils of 30×50 mm^2 area; the uncertainty in the target thicknesses was 1%. They were placed in a movable target holder, which allowed us through two independent rotations to choose the target, and to fix the angle between the target and the beam. Uniform beam illumination of the targets was achieved through their rastering.

2. The positron and electron incident beams

The positron beam was created by the interaction of a 100 MeV electron beam on a 2 mm tungsten radiator located between the sixth and seventh sections of the accelerator. The corresponding positrons, created by pair production, are then accelerated in the 24 remaining sections dephased by π with respect to the first sections. This positron beam could reach a maximum energy of about 500 MeV with an averaged current of about 50 nA.

The positron beam emittance was six times larger than the emittance of the direct electron beam which results in some uncertainty in the absolute normalization of the measurement. This was overcome by taking in addition electron data, at the same beam intensity (30 nA) and with an emittance downgraded to be comparable to that of the positron beam. These data were taken in kinematics previously measured with a small electron emittance [21,22].[2] The ratio of the two electron measurements allows us to normalize our positron data, which can then be safely compared to the small emittance electron data of Refs. [21,22].

The emittance of the electron beam was degraded by installing a 17 μm aluminum foil after the last section of the accelerator. The emittance of the two beams ($\sim2\pi$ mm mrad) was defined by the same mechanical slit system and monitored during the experiment by measuring the beam profiles using a pair of highly sensitive scanning wire systems. The first one, located about 2 m upstream of the target was made out of two perpendicular 300 μm copper wires mounted on a fork. While the scanning system was moved through the beam, secondary emitted electrons produced a signal on the wires that allowed us to reconstruct the beam horizontal and vertical profiles with an accuracy of 0.5 mm. The second monitor was located 7.8 m downstream of the target in front of the Faraday cup. An array of 16 horizontal and 16 vertical wires of 300 μm copper wires measured the beam profile with an accuracy of 1 mm.

We found that, due to misalignment in the beam tuning, our beam spots were positioned about 5 mm under the intersection of the line defined by the center of rotation of the spectrometer and the central ray of the spectrometer collimator. This brings corrections of 0.5% on the solid angle for both spectrometers and 6×10^{-4} on the momentum reconstructed in the electron spectrometer.

Special care was taken to measure the small $\simeq$30 nA beam current. The water used to cool the Faraday cup induced a leakage current similar in magnitude to our mean beam current. By draining and drying the Faraday cup, its leakage current was reduced to $\simeq$30 pA. A ferrite-core induction monitor located upstream of the target provided a redundant charge determination. The charge measurements of the Faraday cup and the ferrite-core monitor were in agreement within 2%.

3. The spectrometer detectors

The HE1 hall contains two magnetic spectrometers:

The SPR600 magnetic spectrometer [23] with momentum acceptance $\Delta P/P_0=35\%$, intrinsic resolution $\delta P/P_0=4\times10^{-4}$ and maximum momentum of 630 MeV/c was equipped with a detector consisting of (i) three planes (R, Y, and T) of plastic scintillators, (ii) a gas Cerenkov counter (C) filled with freon gas (index $n=1.0013$) corresponding to 10 MeV/c electron and 2.7 GeV/c pion thresholds, respectively, and (iii) two multiwire chambers with both horizontal and slanted wires for track reconstruction. The electron trigger was defined by the coincidence RYCT eliminating all pions produced in the target and crossing the detector.

The characteristics of the SPR900 magnetic spectrometer [23] are a momentum range of 9%, intrinsic resolution of 2×10^{-4}, and a maximum momentum of 900 MeV/c. The SPR900 detector package included: (i) two planes (R and Y) of plastic scintillators, (ii) a Čerenkov counter (C) filled with freon gas like that of the SPR600 detector package, and (iii) two multiwire drift chambers with both horizontal and slanted wires for track reconstruction. The electron and/or positron trigger in this detector was defined by the coincidence RYC.

[2]For ^{12}C the measurements were performed at 401 and 440 MeV at 60°.

The SPR600 was used to detect the scattered electrons or positrons within a solid angle of 6.8 msr. For each set of kinematics, several magnetic-field settings of the SPR600 were used, each of them covering an electron momentum range $\Delta P/P_0 = 35\%$ with an overlap of 2% between two consecutive settings.

As the SPR600 was used for main data taking, the SPR900 served as a monitor of the luminosity at each beam energy: it was set at a fixed angle of 41° and its magnetic field was tuned to detect elastically scattered electrons (positrons). The ratio $N_{900}/[N_{\rm inc}t]$ (N_{900} is the number of particles detected in the SPR900, $N_{\rm inc}$ is the number of incident particles, t is the target thickness) and was found to be constant within 1% for all runs at a given beam energy.

4. Corrections on the experimental cross sections

The dead-time correction on our experimental cross sections was about 1%. In addition, four other corrections had to be taken into account: radiative corrections, pair annihilation (only for positrons), pion, and pair production. The former will be developed in Sec. II B and the three others were found to be less than 0.1% for the kinematics studied in this experiment [3]. Systematic effects were found to be of about 3% coming from beam intensity monitoring, and from solid angle and target thickness determinations. Statistical uncertainties ranged between 1.5 to 2% for 5 MeV bins. We have also added quadratically an error equal to 10% on the value of the elastic tail (see Sec. II B 1).

B. Radiative effects

Radiative effects come from the energy-loss processes which occur along the trajectory of the incoming and outgoing particles before, during, and after the scattering. They are divided into two classes: (i) internal corrections which occur during the large angle scattering on the target nucleus, and (ii) external corrections which are due to radiative processes on the other nuclei and atoms of the target. Both classes include bremsstrahlung due to photon emission induced by the nuclear field. External corrections also include ionization and pair annihilation due to collisions with the atomic electrons along the target. In practice for the beam energies used in this experiment we estimated that the contribution of pair annihilation is negligible compared to that of ionization. Therefore, we have used the Mo and Tsai procedure [24,25] to correct for these effects. To correct an experimental quasielastic spectrum, one must (1) subtract the elastic radiative tail, and (2) unfold the quasielastic spectrum obtained after subtraction of the elastic radiative tail.

1. Elastic radiative tail

Since the elastic form factors of lead and carbon vary very rapidly with momentum transfer, the PWBA and the EMA are not good enough to evaluate the elastic electron (positron) cross sections. We have calculated the elastic tails with a phase-shift code using the charge densities compiled by de Vries *et al.* [26] for ^{208}Pb and Reuter *et al.* [27] for ^{12}C. We estimate that the accuracy of this calculation is $\simeq 10\%$.

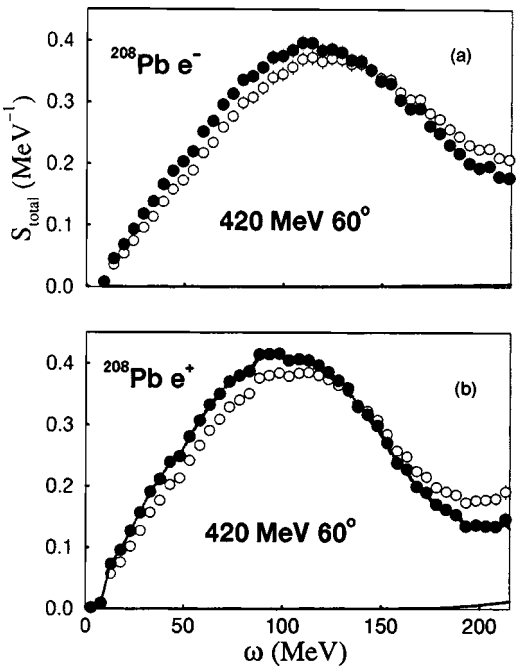

FIG. 1. Experimental spectra after subtraction of the elastic tail for the kinematics ^{208}Pb 420 MeV-60° for electrons (a) and positrons (b); before radiative corrections in the continuum (open circles), after radiative corrections in the continuum (full circles); the solid line represents the elastic tail. For positrons we also show, as discussed in Sec. II B 2, the spectra resulting from radiative corrections obtained with modeled positron cross sections increased by 20% (dotted-dashed line), or with $|V_C| = 25.9$ MeV (dotted line); the difference between these two curves is very small and cannot be distinguished in the figure.

2. Radiative corrections in the continuum

After subtraction of the elastic tail, we unfolded the resulting spectrum. We used the method developed by Miller [28]: the quasielastic peak is divided into a sum of discrete peaks as detailed in Ref. [3]. To unfold the data at a given angle and incident energy E_0, we need the values of the cross section at the same angle and at incident energies $E_i < E_0$. The required electron cross sections were obtained from the previous data [21,22]. In the positron case, the EMA approximation was used to deduce the required positron cross sections at $E_i(e^+) < E_0(e^+)$ from the electron cross sections, i.e., $S_{e^+}(E_i, \omega, \theta) = S_{e^-}(E_i - 2|V_C|, \omega, \theta)$

Since in practice the value of V_C is not known at the beginning of the analysis, we have used an iterative procedure. The positron spectrum was first unfolded using as a first guess for V_C the value of the potential at the center of the nucleus, calculated with the tabulated nuclear charge distribution [26,27]: $|V_C| = 25.9$ MeV for ^{208}Pb and $|V_C| = 4.6$ MeV for ^{12}C. The resulting positron spectrum was compared to the electron spectra to extract V_C using the procedure described in Sec. III A, giving 18.7 MeV for ^{208}Pb and 5.0 MeV for ^{12}C. Then these values of V_C were used to unfold the positron spectrum gain, giving again 18.7 and 5.0 MeV.

Figures 1 and 2 show, together with the elastic tails, the electron, and positron quasielastic spectra after subtraction of the elastic tail, before and after the unfolding procedure for

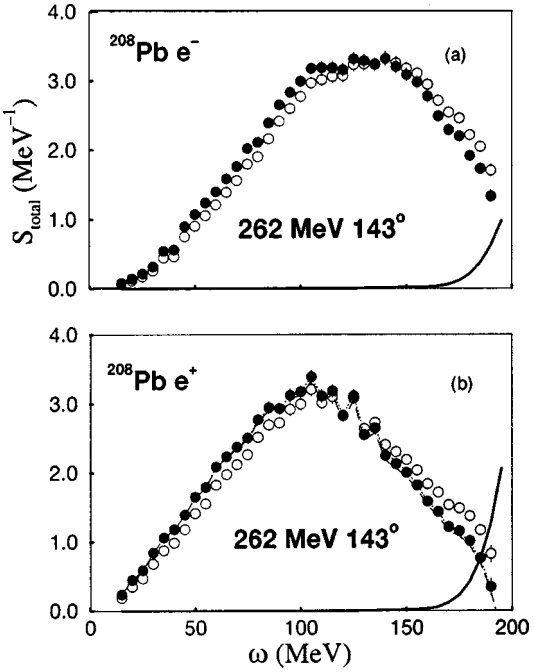

FIG. 2. Same as Fig. 1 for the kinematics ^{208}Pb 262 MeV-143°.

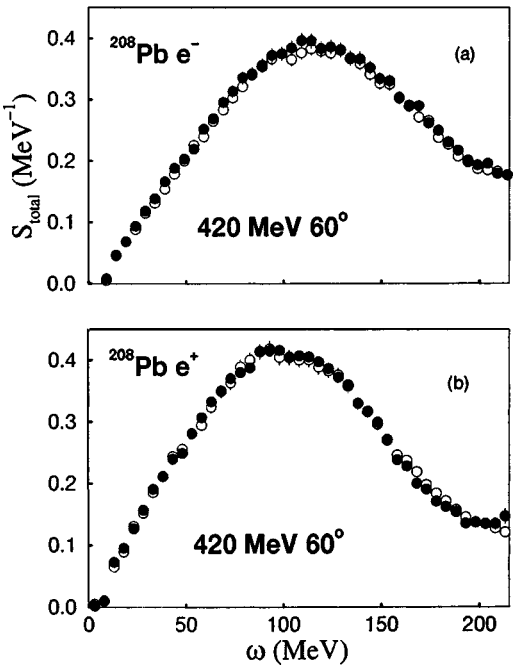

FIG. 3. Comparison of the radiatively corrected electron (a) and positron (b) total responses for the kinematics ^{208}Pb 420 MeV-60° measured with two different target thicknesses, 101 mg/cm^2 (full circles) and 168 mg/cm^2 (open circles).

the two sets of kinematics measured for ^{208}Pb. The unfolded positron spectra using $|V_C|=25.9$ and 18.7 MeV in Figs. 1(b) and 2(b) differ only slightly in the quasielastic peak. This is the reason why the second iteration already gave the same result as the first one.

Furthermore, we can see in Figs. 1(b) and 2(b) that changing the modeled positron cross sections by 20% results in a very small change in the corrected spectrum. As we will see in Sec. III, the EMA is valid within a few percent for the quasielastic cross sections, so that our procedure appears to be safe.

To check the validity of the external corrections, we measured the same ^{208}Pb kinematics (420 MeV-60°) with two target thicknesses, 101 and 168 mg/cm^2. The spectra after subtraction of the elastic radiative tails and continuum corrections are shown in Figs. 3(a) (electrons) and 3(b) (positrons). The corrected spectra are in agreement within the experimental errors. We show in Figs. 4(a) and 4(b) the spectra before and after the radiative corrections unfolding procedure for electrons and positrons scattering off ^{12}C.

III. ANALYSIS AND RESULTS

A. Disentangling Coulomb effects: an experimental procedure

If EMA is a good approximation, we must obtain the same total response function for positrons at an incident energy E_{e^+} and for electrons at an incident energy $E_{e^-}=E_{e^+}-2|V_C|$. The exact value of $|V_C|$ is unknown and has to be determined experimentally. We searched for the best matching between the positron and the electron responses, allowing for two parameters: the incident electron energy E_{e^-} and in addition a constant normalization factor N by which we multiply the electron response. This renormalization factor is an approximation of possible Coulomb distortion effects beyond EMA, but more generally, Coulomb distortions could also induce a deformation of the response function.

At a given kinematic, we proceeded as follows:

(i) S_{total} was extracted from the positron data.

(ii) We compared the positron response to the electron responses obtained at the same angle but at different incident energies. This was possible because electron quasielastic

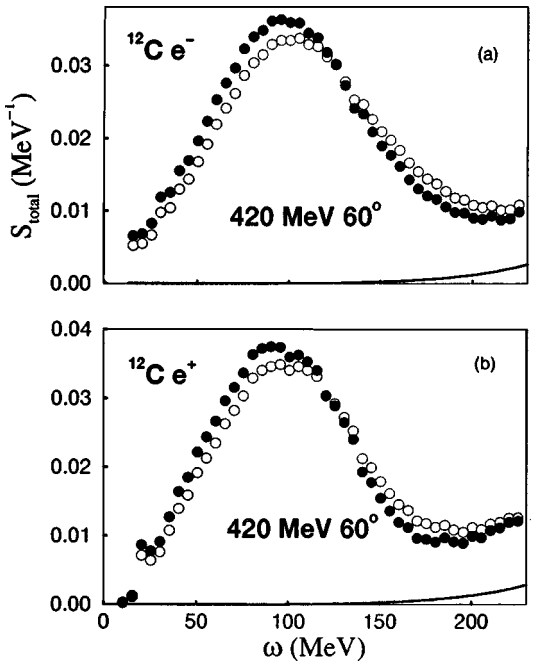

FIG. 4. Same as Fig. 1 for the kinematics ^{12}C 420 MeV-60°.

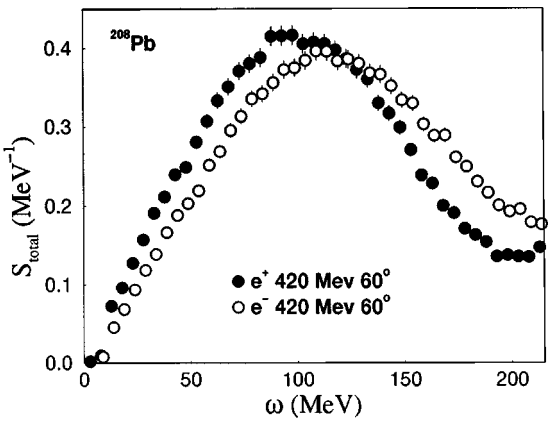

FIG. 5. Positron and electron response functions for the kinematics ^{208}Pb 420 MeV-60°.

data are available for both ^{12}C [21] and ^{208}Pb [22] over a wide range of incident energies at the same angle. An interpolation procedure allowed us to find the incident electron energy E_{e^-} whose response corresponds to the optimal matching between the positions of the electron and positron quasielastic peaks. We chose paths of interpolation which connect the maxima as well as the minima of the measured response functions, and in between, we followed the paths of the constant ratio between maximum and minimum.

Finally, the electron energy E_{e^-} and the relative normalization factor N of the electron and positron spectra are varied to minimize the χ^2 between the two responses. The experimental value of the effective Coulomb potential energy is then obtained as

$$|V_C| = (E_{e^+} - E_{e^-})/2.$$

If EMA is a good approximation, we must find a good matching between the two spectra and a value of N compatible with unity. In addition, the value of V_C for different kinematics on the same target should be the same. The remaining differences between the positron and electron responses, if any, are due to higher-order effects (focusing).

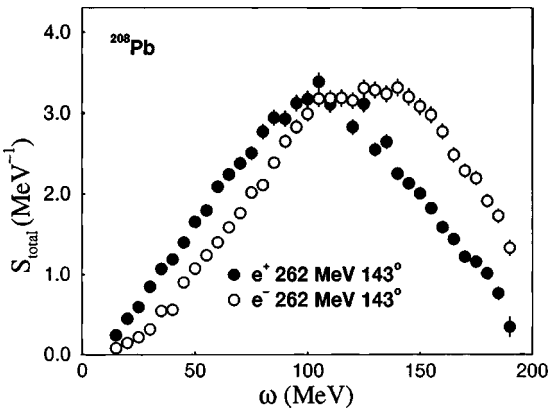

FIG. 6. Positron and electron response functions for the kinematics ^{208}Pb 262 MeV-143°.

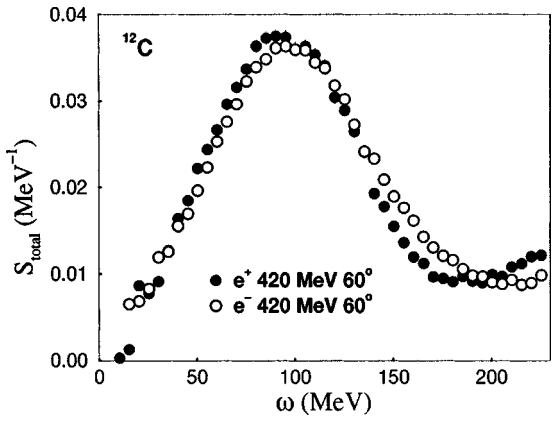

FIG. 7. Positron and electron response functions for the kinematics ^{12}C 420 MeV-60°.

B. Experimental results

Figures 5, 6, and 7 show the electron and positron response functions after radiative corrections for the two ^{208}Pb and the ^{12}C kinematics. We observe a shift between the electron and positron responses which increases with the nucleus charge.

Figures 8, 9, and 10 present the positron response functions for the three kinematics, together with the electron responses which result from the fitting procedure described in Sec. III A, i.e., at incident energies $E_{e^+} - 2|V_C|$ and normalized by the factor N. We note an overall fair agreement between the positron and electron responses.

The results of the Coulomb potential determination are summarized in Table I for all the kinematics. For ^{208}Pb the V_C values obtained for the two kinematics covered by this

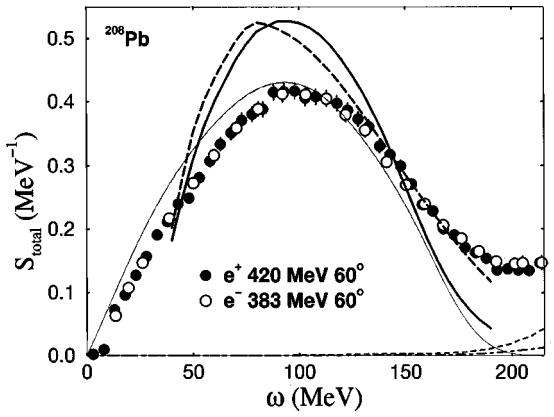

FIG. 8. Positron experimental response function for the kinematics ^{208}Pb 420 MeV-60° (full circles) compared to the electron response function at $E_{e^-} = E_{e^+} - 2|V_C| = 383$ MeV normalized by the factor $N = 1.04$ (open circles). The positron elastic tail is at 420 MeV (dotted-dashed line), the electron elastic tail is at 383 MeV (dashed line). Calculations by the Ohio group [14] are shown for positron at 420 MeV (thick solid line) and for the electron at 383 MeV (thick dashed line). Calculations by Traini *et al.* [12] are shown for a positron at 420 MeV (thin solid line) and for electron at 383 MeV (thin dashed line). The difference between the thin solid and thin dashed lines is very small and cannot be distinguished in the figure.

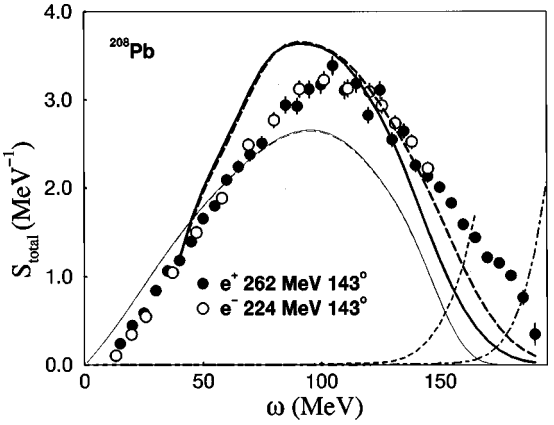

FIG. 9. Same as Fig. 8 for the kinematics ^{208}Pb 262 MeV-143°, $E_e^- = 224$ MeV and $N = 1.02$.

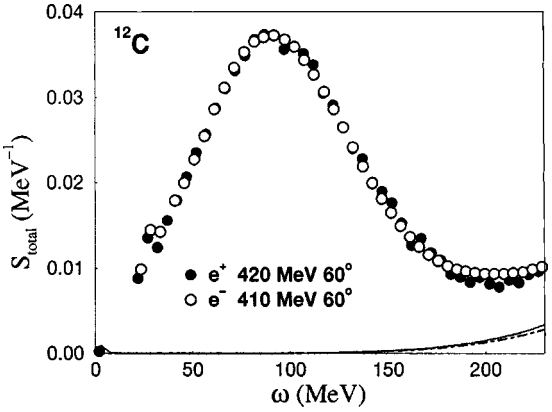

FIG. 10. Positron experimental response function for the kinematics ^{12}C 420 MeV-60° (full circles) compared to the electron response function at $E_{e^-} = E_{e^+} - 2|V_C| = 410$ MeV normalized by the factor $N = 1.02$ (open circles). The positron elastic tail is at 420 MeV (dotted-dashed line), and the electron elastic tail is at 410 MeV (dotted line).

experiment agree within 1σ; the average value is $|V_C| = (18.7 \pm 1.5)$ MeV. For ^{12}C, we find $|V_C| = (5.0 \pm 1.5)$ MeV. The uncertainty in our results includes the experimental errors and the uncertainties of our analysis (statistics, radiative corrections, interpolation . . .).

The fact that the positron responses on ^{208}Pb, for kinematics which differ in incident energies and angles, can be matched with electron responses with the same value of V_C and a value of N close to unity is a strong indication of the validity of the EMA.

We can parametrize the Coulomb potential. If we assume that it has the form [20]

$$|V_C| = \frac{KZ}{\langle r^2 \rangle^{1/2}}, \tag{8}$$

the best fit of our experimental results on ^{208}Pb and ^{12}C gives

$$|V_C| = \frac{(1.27 \pm 0.10)\ (\text{MeV fm})}{\langle r^2 \rangle^{1/2}} Z, \tag{9}$$

using the values $\langle r^2 \rangle^{1/2} = 2.47$ fm for ^{12}C and 5.5 fm for ^{208}Pb given by de Vries *et al.* [26]. The values of the Coulomb potential obtained with Eq. (9) are $|V_C|_{\text{fit}} = (3.1 \pm 0.25)$ MeV for ^{12}C and $|V_C|_{\text{fit}} = (18.9 \pm 1.5)$ MeV for ^{208}Pb.

These values are smaller than the values at the origin ($|V_C(0)| = 4.6$ MeV for ^{12}C and $|V_C(0)| = 25.9$ MeV for ^{208}Pb) computed using the charge distributions determined experimentally [19,27] but agree with the average potential computed according to the following equation:

$$|V_C| = \frac{\int \rho(r) |V_C|(r)\, d^3r}{Z|e|}, \tag{10}$$

using the same charge distribution.

We give in Table II the parametrized value of $|V_C|$ for several nuclei [Eq. (9)] together with the average potential calculated with the experimental charge distribution using Eq. (10); they agree within the error bars.

C. Comparison with theory

We compare our electron and positron experimental response functions for ^{208}Pb with the calculation of Traini *et al.* [12] in Figs. 8 and 9. This theoretical model takes into account Coulomb distortion effects by including the EMA and higher-order focusing effects, using for V_C the effective value obtained in the present experiment. The model, however, does not include meson exchange current and isobar configuration contributions. It reproduces qualitatively the position and the width of the total response in the quasielastic region for both electrons and positrons. For $\omega > \omega_{\text{peak}}$, exchange currents and pionic degrees of freedom become important and a large discrepancy appears.

TABLE I. Experimental Coulomb potential V_C obtained from this experiment. The fitted electron energy E_{e^-} and the normalization factor N are obtained as explained in Sec. III A.

Kinematic	Thickness (mg/cm^2)	N	E_{e^+} (MeV)	E_{e^-} (MeV)	$\lvert V_C \rvert$ (MeV)
^{208}Pb(420 MeV,60°)	101	1.04 ± 0.03	420	383 ± 3	18.5 ± 1.5
^{208}Pb(420 MeV,60°)	168	1.04 ± 0.03	420	383 ± 3	18.5 ± 1.5
^{208}Pb(262 MeV,143°)	168	1.02 ± 0.03	262	224 ± 3	19.0 ± 1.5
^{12}C(420 MeV,60°)	499	1.02 ± 0.03	420	410 ± 3	5.00 ± 1.5

TABLE II. Coulomb potential energies of several nuclei evaluated using the experimental charge densities of Ref. [26]. Both the Coulomb potential at the origin $|V_C(0)|$ and its averaged value $|V_C|$ from Eq. (10) are shown. The values of the fit of Eq. (9) are also shown together with the experimental charge mean-square radii.

Nucleus	$\langle r^2\rangle_{\rm exp}^{1/2}$ (fm)	$\lvert V_C(0)\rvert$ (MeV)	$\lvert V_C\rvert$ (MeV)	$\lvert V_C\rvert_{\rm fit}$ (MeV)
^{12}C	2.464	4.6	3.3	3.1 ± 0.25
^{40}Ca	3.450	10.5	7.9	7.4 ± 0.6
^{48}Ca	3.451	10.4	7.9	7.4 ± 0.6
^{56}Fe	3.714	12.5	9.5	8.9 ± 0.7
^{90}Zr	4.258	16.7	12.8	11.9 ± 0.9
^{154}Gd	5.124	21.8	16.9	15.9 ± 1.2
^{208}Pb	5.503	25.9	20.1	18.9 ± 1.5

The level of agreement in the quasielastic region is sufficient for a reliable estimation of Coulomb distortion effects in this region. The model predicts higher-order Coulomb effects smaller than 1% separately for e^+ and e^-; in particular the difference between the positron response at E_{e^+} and the electron response at $E_{e^+}-2|V_C|$ can hardly be seen in Figs. 8 and 9. This is in agreement with our experiment.

The validity of the EMA for the quasielastic scattering is not surprising. As mentioned in the introduction the EMA neglects the variation of V_C. This is an approximation whose quality depends on how much the nucleon response varies with V_C. This is confirmed by the analytical approach of Ref. [12] where the size of the focusing effects is related to the derivatives of the Born amplitude with respect to the kinematical variables. In elastic scattering the derivatives can be quite large due to the presence of diffraction minima resulting in changes of the total response by orders of magnitude. The same thing occurs in $(e,e'p)$ reactions where the cross section depends strongly on the so-called recoil momentum. In contrast, the inclusive response varies quite smoothly in the quasielastic region. In particular the momentum transfer dependence is essentially the relatively smooth dependence of the proton elastic form factors. A small contribution of focusing effects is then expected in inclusive quasielastic experiments.

We recently published [22] the results of a quasielastic inclusive experiment on ^{208}Pb. In the analysis we used the Coulomb corrections from Ref. [5] which were estimated in the same framework as Ref. [12]. However, due to oversimplified transition densities the nuclear model used in Ref. [5] does not reproduce the width of the quasielastic peak, and overestimates the derivatives of the response. As a consequence the Coulomb corrections are also overestimated, and a reanalysis will be performed [29].

Figures 8(a), 8(b), and 9 also display the predictions of the Ohio group [14]. These predictions point to large focusing effects since they are quite different for electrons and positrons. This is in clear disagreement with our measurements.

IV. CONCLUSION

Electron and positron quasielastic cross sections on ^{12}C and ^{208}Pb were measured and compared in order to study Coulomb distortion effects. A particular stress was put on checking the validity of the effective momentum approximation (EMA). In this approximation the incoming and outgoing leptons are still represented by plane waves associated to an effective energy which differs from the actual energy by an effective Coulomb potential energy V_C. The resulting electron and positron response functions at the same effective kinematics are identical within the experimental error bars.

The best fit between the electron and positron responses was determined allowing two free parameters, V_C and a relative normalization factor. A good match is found and the renormalization factor is compatible with unity within a 3% experimental uncertainty. In addition, values of V_C obtained for different kinematics appear to be compatible, and we find $|V_C|=(5\pm1.5)$ MeV for ^{12}C and (18.7 ± 1.5) MeV for ^{208}Pb, consistent with the average value of the Coulomb potential within the nuclear volume. These results constitute a strong support for the EMA in inclusive quasielastic scattering.

Our results are in good agreement with Ref. [12] which predicts indeed very small distortion effects beyond EMA for inclusive quasielastic experiments. They clearly disagree with Ref. [14] where a large difference between electron and positron responses at the same effective kinematics is predicted.

[1] V. Breton *et al.*, Phys. Rev. Lett. **66**, 572 (1991).
[2] P. Guèye *et al.*, Phys. Rev. C **57**, 2107 (1998).
[3] P. Guèye, Ph.D. thesis, Université Blaise Pascal, Clermont Ferrand, 1994.
[4] C. Giusti and F. D. Pacati, Nucl. Phys. **A473**, 717 (1987); **A485**, 461 (1988); C. Giusti, S. Boffi, and F. D. Pacati, Phys. Rep. **226**, 1 (1993).
[5] M. Traini and S. Turck-Chièze, Proceedings of the Fifth Mini-Conference, Amsterdam, 1987, p. 124; M. Traini, S. Turck-Chièze, and A. Zghiche, Phys. Rev. C **38**, 2799 (1998).
[6] J. P. Dermott, Phys. Rev. B **65**, 1991 (1990).
[7] D. Onley, Y. Jin, and E. Wright, Phys. Rev. C **45**, 1311 (1992); **50**, 168 (1994).
[8] J. M. Udìas *et al.*, Phys. Rev. C **51**, 3246 (1995).
[9] V. Van der Sluys, K. Heyde, J. Ryckebusch, and M. Waroquier, Phys. Rev. C **55**, 1982 (1997).
[10] G. Co' and J. Heinseberg, Phys. Rev. B **197**, 489 (1987).
[11] M. Traini, Phys. Lett. B **213**, 1 (1988).
[12] M. Traini and M. Covi, Nuovo Cimento A **108**, 723 (1995); M. Traini, *ibid.* **108**, 1259 (1995).
[13] Yanhe Jin, Ph.D. thesis, Ohio University, 1991.
[14] D. Onley, Y. Jin, and E. Wright, Phys. Rev. C **45**, 1333

(1992); K. S. Kim, L. E. Wright, Y. Jin, and D. W. Kosik, *ibid.* **54**, 2515 (1996).
[15] D. J. Engel, Phys. Rev. C **57**, 2004 (1998).
[16] D. R. Yennie, F. L. Boos , Jr., and D. G. Ravenhall, Phys. Rev. **137**, 882 (1965).
[17] F. Lenz and R. Rosenfelder, Nucl. Phys. **A176**, 513 (1971).
[18] J. Knoll, Nucl. Phys. **A201**, 289 (1973); **A223**, 462 (1974).
[19] B. Frois *et al.*, Phys. Rev. Lett. **38**, 152 (1977).
[20] R. Rosenfelder, Ann. Phys. (N.Y.) **128**, 188 (1980).
[21] P. Barreau *et al.*, Nucl. Phys. **A402**, 515 (1983).
[22] A. Zghiche *et al.*, Nucl. Phys. **A572**, 313 (1994); **A584**, 757 (1995).
[23] P. Leconte *et al.*, Nucl. Phys. **401**, 169 (1980).
[24] L. W. Mo and Y. S. Tsai, Rev. Mod. Phys. **41**, 205 (1969).
[25] Y. S. Tsai, Rev. Mod. Phys. **46**, 815 (1974).
[26] H. de Vries *et al.*, At. Data Nucl. Data Tables **36**, 495 (1987).
[27] W. Reuter *et al.*, Phys. Rev. C **26**, 806 (1982).
[28] G. Miller, SLAC report 129 (1971).
[29] J. Morgenstern, Internal report of CEA-Saclay, DAPNIA-SPHN-99-30 (1999).